

AD-A056 455

ARMY ENGINEER WATERWAYS EXPERIMENT STATION VICKSBURG MISS F/G 13/13
RESPONSE OF SHALLOW-BURIED STRUCTURES TO BLAST LOADS, (U)
JUN 78 S A KIGER, J P BALSARA

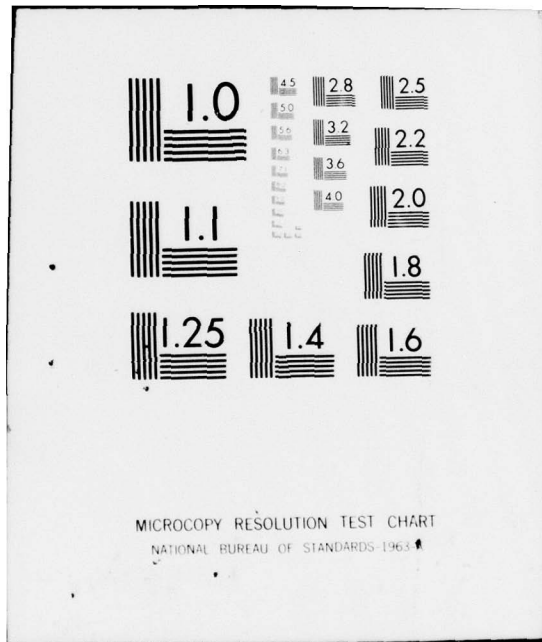
UNCLASSIFIED

NL

| OF |
AD
A056455



END
DATE
FILED
8-78
DDC



MICROCOPY RESOLUTION TEST CHART
NATIONAL BUREAU OF STANDARDS-1963

AD No. 1
DC FILE COPY

ADA056455

*KIGER & BALSARA

LEVEL II

1

(11) Jan 78

(12) 1/14 p.

6

RESPONSE OF SHALLOW-BURIED STRUCTURES TO BLAST LOADS

JUN 1978

(10) SAMMY A./KIGER
JIMMY P./BALSARA
U. S. ARMY ENGINEER
WATERWAYS EXPERIMENT STATION
VICKSBURG, MISSISSIPPI 39180

D D C

REF ID: A64914
JUL 12 1978
RECEIVED
D
50

Hardness levels of shallow-buried structures for vulnerability studies are primarily obtained from calculations using an undamped single-degree-of-freedom (SDOF) elastic-plastic model. Recent and past tests on buried structures have shown that the response has, in general, been overpredicted by both the SDOF model and by more exact analyses. In fact, no fully buried concrete structure has collapsed when exposed to simulated or actual nuclear airblast loading, with a number of structures retaining their protective capability at overpressures higher than their predicted collapse load.

Accurately predicting the response of a buried structure is complicated by the fact that the actual loading on the structure is determined in a complex manner by the response of the structure. Unlike the loads normally assumed in the analysis of surface structures, which are essentially unchanged by structural deformations, the loads acting on a buried structure are extremely sensitive to relatively small structural deformations. The differences in experimental results and calculations are attributed to insufficient knowledge of the load distribution acting on the buried structure and neglect of the influence of damping that results from structural deformation, hysteresis in soils, stress wave radiation into the soil, and shear friction at the soil-structure interface.

The Weapons Effects Laboratory at the U. S. Army Engineer Waterways Experiment Station (WES) has recently been conducting tests and analyses of shallow-buried structures to determine the influence of soil cover on the load transmitted to the structure, their static resistance and ductility, and their failure modes under static and dynamic

78 06 09 097

DISTRIBUTION STATEMENT A
Approved for public release;
Distribution unlimited

038 104

1 JUN

*KIGER & BALSARA

loading. Results of this program are being used to evaluate and modify the SDOF model for vulnerability analysis.

This paper summarizes the results from three tests conducted on reinforced-concrete box-type structures and discusses the implications of these test results on current vulnerability calculations.

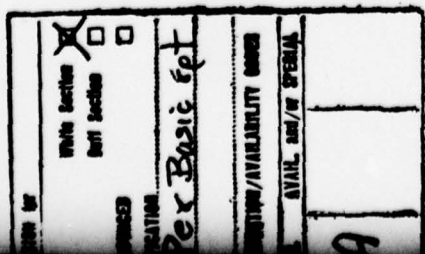
Static Test Results. The objective of the static test was to experimentally determine the load-deflection behavior of the buried structure and to examine the soil-structure interaction phenomena up to the point of structural collapse. The test was conducted in the Large Blast Load Generator Facility located at the WES, Vicksburg, MS. The structure was placed in the facility and covered with sand to a depth of 1 foot. A rubber membrane was then placed over the surface of the sand, and water was pumped in to slowly apply pressure to the soil-structure system until failure occurred.

The test structure was of reinforced-concrete slab type construction where the roof, floor, and wall slabs had span-to-depth ratios of 10. The structure was 8 feet long by 2 feet high by 2 feet wide (inside dimensions). The overall wall thickness, including 0.5 inches of concrete cover on the reinforcing steel, was 2.9 inches. Principal reinforcing was 1 percent tension and 1 percent compression with approximately 1.5 percent shear reinforcement.

Figure 1 shows the load-deflection curve for the soil-structure system. The static water pressure is plotted on the vertical axis, and the roof deflection at the center of the structure is plotted on the horizontal axis. The maximum pressure sustained by the soil-structure system was about 640 psi. However, the maximum flexural capacity for the two-way roof slab assumed rigidly fixed at all edges, is a uniform pressure of 107 psi (Reference 1).

$$P_f = 107 \text{ psi} \quad (1)$$

Soil arching, defined as the ability of a soil to transfer loads from one location to another in response to a relative displacement between locations, is primarily responsible for the increase in capacity from 107 psi to 640 psi. Embedded structures that are much stiffer than their surrounding medium will tend to attract load. On the other hand, stresses will be diverted away from or around embedded structures that are less stiff than their surrounding medium. The redistribution of load is called "passive arching" when the structure is loaded above the free-field stress and "active arching" when the stresses on the structure are less than the free-field stress. An



78 06 09 097

*KIGER & BALSARA

excellent discussion of the soil arching phenomena can be found in Reference 2.

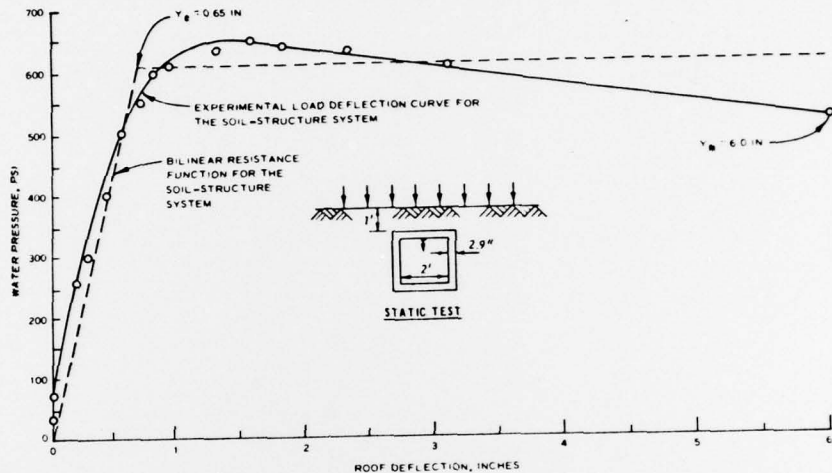


Figure 1. Resistance curves for the soil-structure system.

The pressure acting on the roof and side of the structure when the water pressure was 640 psi is shown in Figure 2. This interface pressure distribution was approximated by fitting a parabola through data taken from interface pressure gages located at each edge of the roof, the center of the roof, the top of the sidewall, and the center of the sidewall. Passive arching over the relatively stiff walls of the structure has acted to increase the pressure to over 800 psi (calculated by extrapolating the parabola). However, active arching over the flexible center of the roof has decreased the pressure to approximately 100 psi. This shift of pressure away from the center of the span toward the supports effectively decreases the maximum bending moment in the structure, and can significantly increase the resistance of the structure to the applied overpressure.

Inplane forces produced by lateral earth pressure is partly responsible for the increased structural capacity. From Figure 2, the thrust in the roof is 2800 lb/in. The moment-thrust interaction diagram shown in Figure 3 was computed using a representative cross section of the roof slab. At 2800 lb/in. of thrust, the moment necessary to form a hinge is approximately 5800 in.-lb/in. Therefore, the uniform pressure required to fail the roof, i.e., to form hinges

*KIGER & BALSARA

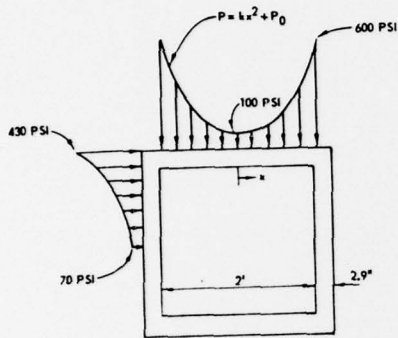


Figure 2. Interface pressure distribution at maximum surface pressure.

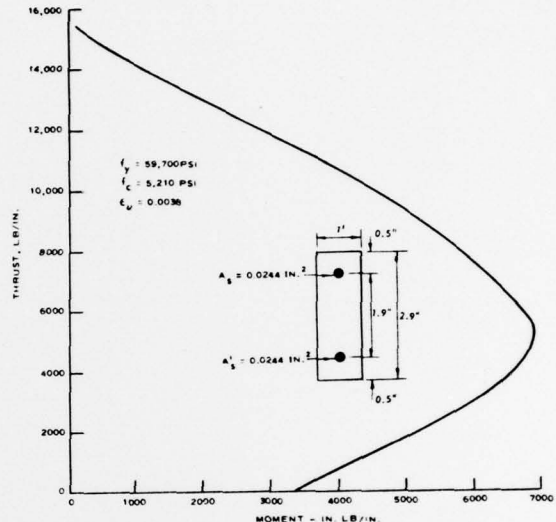


Figure 3. Moment-thrust interaction diagram.

at each support and the center of the roof, is 160 psi. Thus, the flexural capacity of the roof including inplane forces is 160 psi.

In order to compare the computed capacity to the maximum pressure actually sustained by the roof, an "equivalent" uniform load will be computed based on similar moment distributions. From Figure 2, the fixed-end moment produced by the parabolic pressure distribution on the roof is approximately 9600 in.-lb/in. This exceeds the moment capacity of 5800 in.-lb/in. computed from the moment-thrust interaction diagram in Figure 3. Therefore, assume hinges have been formed at each side of the roof and the moment at each hinge is 5800 in.-lb/in. The moment at the center of the roof in Figure 2 necessary to maintain equilibrium under these conditions is 7400 in.-lb/in. The "equivalent" uniform load that will produce moments of 5800 in.-lb/in. at each end and 7400 in.-lb/in. at the center of the roof is 183 psi. Clearly, the inplane loading did act to increase the ultimate capacity. However, the redistribution of the pressure on the roof due to soil arching is primarily responsible for increasing capacity from the 107 psi in Equation 1 to the measured 640-psi peak pressure.

Most "first-cut" design and targeting analysis procedures are based on an undamped SDOF model using a bilinear resistance function. The bilinear resistance for the soil-structure system as approximated

*KIGER & BALSARA

from the experimental load-deflection data is shown in Figure 1. Elastic behavior is assumed up to a deflection, Y_e , and fully plastic behavior is then assumed until failure at the maximum deflection, Y_m . The ductility μ is defined by $\mu = Y_m/Y_e$. From Figure 1, the ductility is about 9.

A standard calculation for the ductility involves calculating the elastic deflection and assuming a maximum deflection. The elastic deflection is a function of the slope of the elastic portion of the resistance function, i.e., its stiffness, and the ultimate static capacity, i.e., the pressure at the onset of plastic deflection. From Biggs (Reference 3), the effective stiffness of a fixed-fixed beam of unit width representing the roof slab is

$$K_e = \frac{307EI}{L^4} = 2650 \text{ psi/in.}$$

where I is the average moment of inertia for cracked and uncracked sections. From Equation 1, the flexural capacity of the roof is about 107 psi. Thus, the elastic deflection, $Y_e = P_f/K_e = 0.04$ in. If a failure deflection of 6 inches is assumed, then the ductility is 150. Clearly, defining a "failure ductility" can be very difficult. Unfortunately, most vulnerability analyses currently define failure in terms of ductility.

In Reference 4, Cooper suggests defining failure in terms of specific energy absorbed to failure and shows that, if $e = \text{constant}$ is taken as a measure of failure, then μ and T (or μ and K) are related by

$$\mu T^2 = \text{constant}$$

or

$$\mu/K = \text{constant}$$

where T is the natural period and K is the stiffness. Therefore, if a given ductility is defined as failure, then errors in T or K can lead to significant errors in failure estimates.

Dynamic Test Results. Two high-explosive (HE) simulation tests were conducted. The first experiment used 21-pound spheres of TNT buried to midstructure depth to simulate the explosive effect of a

*KIGER & BALSARA

5000-pound general purpose bomb penetrating the soil overburden and exploding at midstructure depth. The second experiment employed a foam HEST (high-explosive simulation technique) test to simulate the overpressure from a 1-kt nuclear device at the 2000-psi overpressure range.

Both tests employed identical model structures which were twice the scale of the model used in the static test. They were reinforced-concrete slab-type models with roof, floor, and wall span-to-depth ratios of 10. The structures were 16 feet long by 4 feet high by 4 feet wide (inside dimensions). The overall wall thickness, including 0.8 inches of cover on the reinforcing steel, was 5.6 inches. Principal reinforcing steel was 1 percent tension and 1 percent compression with approximately 1.5 percent shear reinforcement. These models are approximately 1/4-scale models of a typical hardened shallow-buried structure. A more complete description of the model structure, including construction drawings, is given in Reference 5.

21-Pound HE Test Results. The model structure was covered to a depth of 2 feet for the test. Three 21-pound spherical TNT charges were used. The charges were buried to midstructure depth and detonated

at 8 feet, 6 feet, and 4 feet from the structure wall. A schematic drawing of the test configuration is shown in Figure 4. No damage resulted from the charge at 8 feet. With the charge at 6 feet, flexural cracking occurred but no measurable permanent deflection of the wall could be found. The test at 4 feet was conducted on the opposite side of the structure on the undamaged

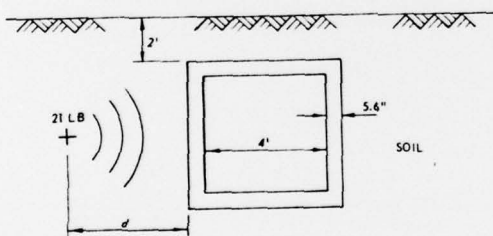


Figure 4. Test configuration for 21-pound HE test.

wall. Structural damage resulting from the detonation at 4 feet is shown in Figure 5. Posttest measurements indicated approximately 10.5 inches of permanent deflection at the center of the wall. There were no interface pressure records obtained in this experiment; however, the pressure record measured at the soil-structure interface in a test using an identical HE charge in the same soil on a structural model with 13-inch-thick walls is given in Figure 6 and will be used in the SDOF analysis.

HEST Test Results. The foam HEST used in this study can accurately simulate the overpressure component of the airblast generated by a nuclear detonation. This test allows a large area to be

*KIGER & BALSARA

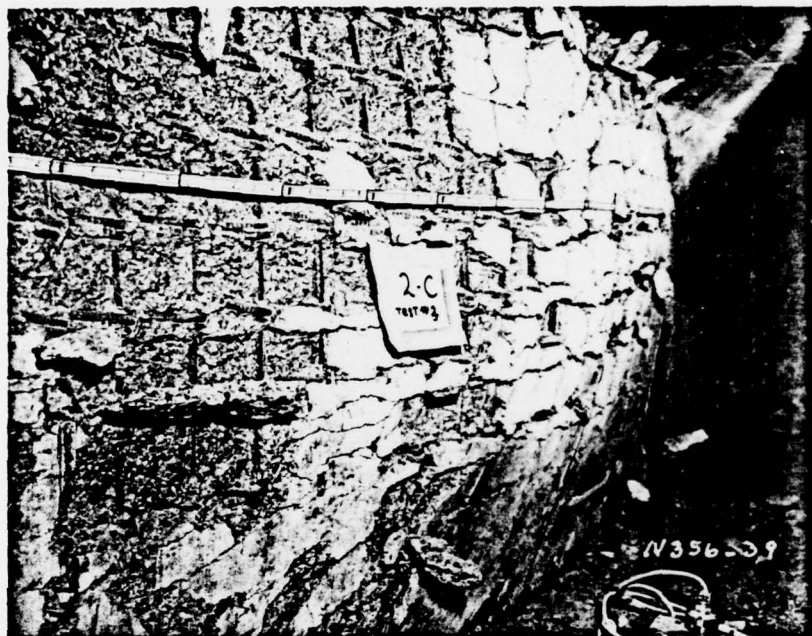


Figure 5. Structural damage from a 21-pound TNT subsurface detonation at 4 feet from the wall.

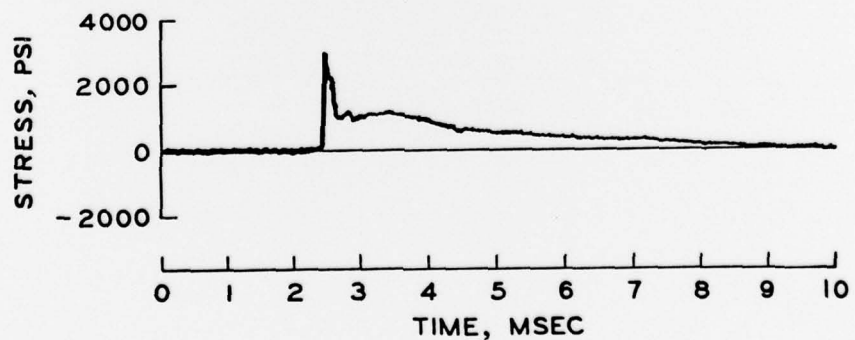


Figure 6. Soil-structure interface pressure from a 21-pound TNT subsurface detonation at 4 feet from a rigid wall.

exposed to a uniform pressure level and gives pressure durations long enough to simulate the impulse associated with a nuclear event.

*KIGER & BALSARA

The foam HEST configuration used for this test is shown in Figure 7. The 6-inch charge cavity is filled with Styrofoam and evenly distributed strands of detonating chord. A charge density of 0.914 pound of explosive per square foot was used to produce a peak pressure of approximately 2000 psi, and the overburden of 32 inches of uncompacted native soil was designed to confine the blast long enough to simulate the pressure duration associated with a 1-kt nuclear device.

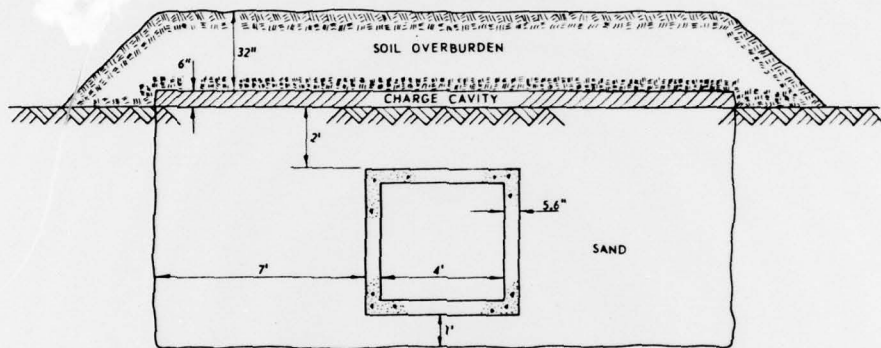


Figure 7. Foam HEST test configuration.

The airblast measured at ground level beneath the charge cavity is shown in Figure 8.

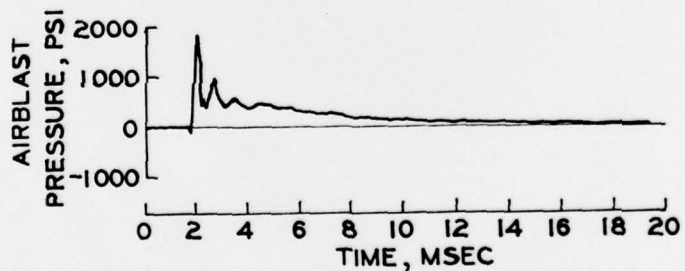


Figure 8. Foam HEST airblast.

Interface pressures measured on the structure are shown in Figure 9. Note that the initial peak pressure is approximately 1200 psi at each edge of the roof (Gages IF1 and IF3) and at the center of the roof (Gage IF2). However, the pressure at the flexible center of the roof is quickly reduced to zero and remains at zero for the duration of the airblast load. This indicates that the soil arching phenomena so important in the static test can be equally important in

*KIGER & BALSARA

the case of dynamic loading. Structural damage from the HEST event was a 0.5-inch permanent deflection at the center of the roof with extensive tensile cracking of the concrete in the roof. Damage to the floor of the structure was very similar to the roof.

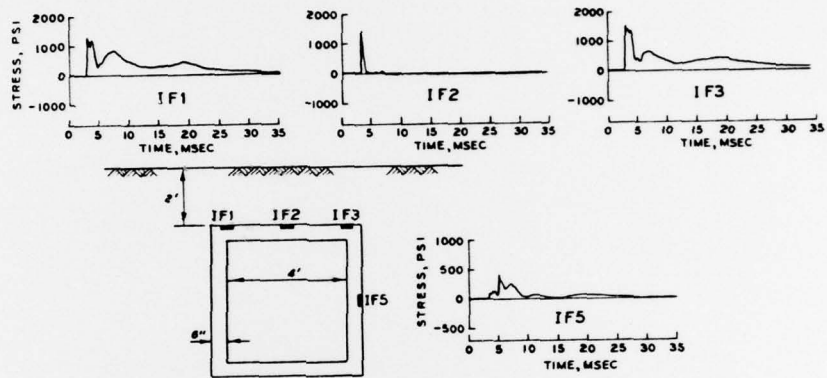


Figure 9. Foam HEST interface pressure records.

Analysis and Discussion of Results. It is assumed that the reader is familiar with the dynamic analysis of structures using a SDOF model. The essential elements of the SDOF model are an equivalent mass and resistance and a damper. Methods for calculating these parameters are given in References 1 and 3. The resistance may be either a linear or nonlinear spring and is normally approximated as a bilinear representation of the static resistance for the structure or structural element being analyzed.

21-Pound HE Test Analysis. The resistance function shown in Figure 10 was approximated from the static test results shown in

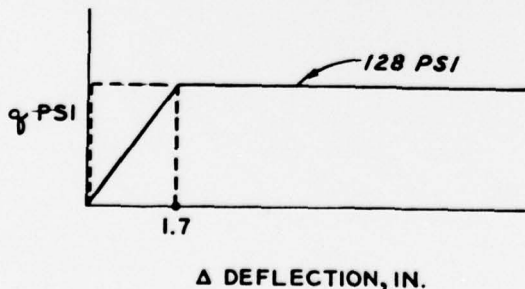


Figure 10. Resistance function for 21-pound HE test analysis.

Figure 1. The elastic deflection in Figure 1 was taken as 0.85 inch and doubled because the static test structure was a 1/2-scale model of the structure used in the 21-pound HE test. The ultimate capacity of the structure as computed using the procedures in Reference 9 is 128 psi. The 128-psi resistance includes some inplane loading but ignores soil arching and was used for the SDOF analysis.

*KIGER & BALSARA

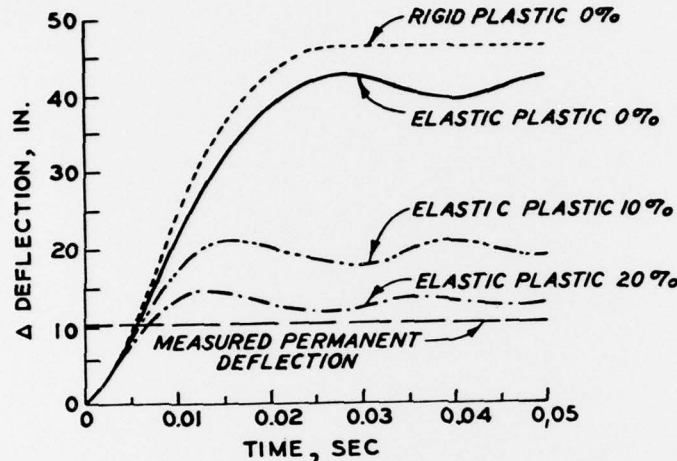


Figure 11. SDOF analysis results for 21-pound test.

shown in Figure 11. The percent numbers shown are the percent of critical damping in the SDOF model. Critical damping is defined as the minimum amount of damping for which no oscillations will occur under free vibration. The dynamic loading used for this analysis is shown in Figure 6. Discussion of the results in Figure 11 will be combined with the discussion of the foam HEST test analysis below.

Foam HEST Test Analysis. Since the surface loading from the foam HEST is a uniform load similar to the static load, it is assumed that the soil-structure interaction phenomena will be similar. This assumption will allow the use of the resistance function developed in the static test and shown as a dotted line in Figure 1 to be used for the SDOF analysis. Note that the displacement scale must be doubled because the static test structure was a 1/2-scale model of the HEST test structure. The loading function for this analysis is the surface airblast loading shown in Figure 8. Results of the SDOF analysis are given in Figure 12. The elastic-plastic calculation with no damping is not included in Figure 12 because it gave a 6-inch maximum deflection and could not conveniently be included on the same graph.

Discussion of Results. The results presented in Figures 11 and 12 both indicate the current vulnerability model, the undamped SDOF model, significantly overpredicts the structural response from both conventional and nuclear type blast loadings. Recent experimental results (Reference 6) and calculational results (References 7 and 8) have indicated that 20 to 25 percent of critical damping is appropriate for this structure in the buried configuration. The results in Figures 11 and 12 indicate that the 20 percent damped SDOF model can accurately predict the structural response. It is important to realize that soil arching and inplane loading were accounted for in the foam

*KIGER & BALSARA

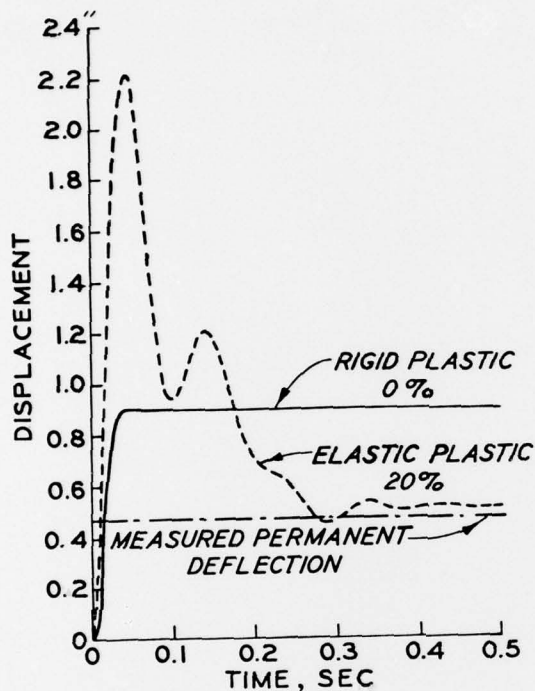


Figure 12. SDOF analysis results for foam HEST test.

calculations represented in Figure 13, failure was taken to be 40 inches of roof deflection (4 times the deflection measured in the 21-pound HE test).

The high shear strength soil curve in Figure 13 was obtained from a 20 percent damped SDOF model assuming the same soil arching and inplane loading as would be expected in a static loading, i.e., using the resistance function in Figure 1 with the displacement scaled by 4. The zero shear strength curve represents a model with no soil arching protection provided, ultimate capacity as computed from Reference 9 at 128 psi, damping at 20 percent of critical, and elastic deflection 4×1.7 inches from Figure 10.

The curve labeled current vulnerability calculations in Figure 13 is based on the SDOF model recommended in Reference 9 with maximum resistance equal 128 psi. This model includes modifying the period to account for soil cover, and applying inplane forces to account for lateral earth pressure. Calculation for the roof load

HEST analysis by using the static resistance function in Figure 1 for the soil-structure system.

Figure 13 quantitatively compares the results from the experiments discussed in this report to calculations based on the most current vulnerability manual available (Reference 9).

The results presented in Figure 13 are based on calculations for a full-scale structure with inside dimensions 16 feet by 16 feet by 64 feet with walls, roof, and floor 23 inches thick (19.2 inches effective depth). The compressive strength of the concrete was 5200 psi, the yield strength of the reinforcement steel was 72,000 psi, and tension and compression reinforcement were each 1 percent. The structure was buried 8 feet deep. For all

*KIGER & BALSARA

includes attenuation of the overpressure with depth; however, Reference 9 includes no damping and, for shallow depths of burial, no soil arching.

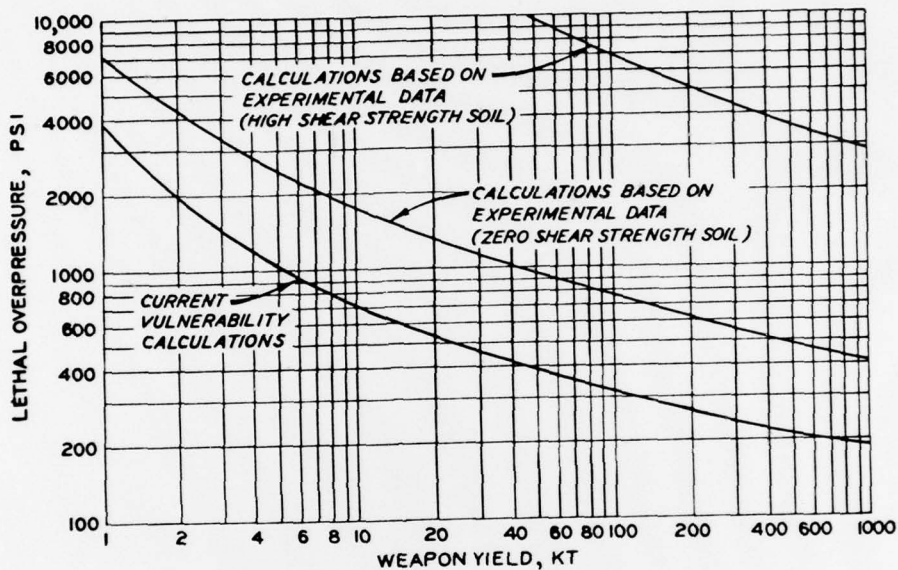


Figure 13. Current vulnerability calculations compared to calculations using a damped SDOF model including soil-structure interaction.

As an example use for the curves in Figure 13, consider the HEST test results described above. The HEST test structure is a 1/4-scale model of the structure calculated in Figure 13. Using cube root scaling (charge weight scales like the cube of length), the 1-kt weapon simulated in the HEST test scales to a 64-kt weapon in Figure 13. The current vulnerability calculations curve indicates failure (40 inches of roof deflection) will occur at 350 psi. The 20 percent damped SDOF model with no soil arching indicates failure at about 900 psi. The experimental results from the HEST test at 2000 psi produced 2 inches of roof deflection (0.5 inch times the scale factor of 4), and the 20 percent damped SDOF model including maximum soil arching indicates failure at the 8500-psi overpressure range from a 64-kt weapon. Based on HEST test results, no damage would be expected at an overpressure of 350 psi and yet the best available vulnerability analysis manual predicts complete structural collapse at 350 psi! Clearly the vulnerability analysis model used for shallow-buried structures needs some

*KIGER & BALSARA

modification. Results from the test described in this report suggest that a damped SDOF model can adequately predict the response of shallow-buried structures to blast loads provided the soil-structure interaction is accounted for when computing the loads on the buried structure.

Conclusions

1. During the static test, inplane forces in the roof slab produced by lateral soil pressure increased the ultimate capacity of the structure from 107 psi to approximately 180 psi.
2. The redistribution of pressure acting on the roof of the structure caused by soil arching in the static test effectively increased the capacity of the soil-structure system to 640 psi.
3. The ductility of the structure as calculated from the load-deflection curve from the static test was approximately 9. However, the ductility is approximately 150 when calculated using the measured 6-inch maximum roof deflection from the static test and computing the elastic deflection from standard design text. Ductility is not a good parameter to use to define failure when large plastic deformations are involved.
4. Soil arching can be ignored when computing structural loads from the localized HE burst associated with conventional weapons. However, soil arching can significantly reduce the loads on a buried structure when the loading is produced by plane waves such as those associated with nuclear airblast. As indicated in Figure 13, the increased capacity due to soil arching may be as much as a factor of 10.
5. The SDOF model for calculating the dynamic response of shallow-buried structures should be damped at approximately 20 percent of critical. Then, if soil arching and inplane forces due to lateral earth pressure are adequately accounted for in computing the loads on the structure, the damped SDOF model can accurately predict the structural response from blast loads.

References

1. R. E. Crawford, C. J. Higgins, and E. H. Bultmann, "The Air Force Manual for Design and Analysis of Hardened Structures," Technical Report No. AFWL-TR-74-102, October 1974, Air Force Weapons Laboratory, Kirtland Air Force Base, NM.

*KIGER & BALSARA

2. J. W. McNulty, "An Experimental Study of Arching in Sand," Technical Report No. 1674, May 1965, U. S. Army Engineer Waterways Experiment Station, CE, Vicksburg, MS.
3. J. M. Biggs, Introduction to Structural Dynamics, 1964, McGraw-Hill Book Company, New York, NY.
4. H. F. Cooper, Jr., E. J. Chapyak, and K. Y. Narasimhan, "A Parametric Study of Hard Structure Survival to Nuclear Overpressure Loading," Technical Report No. RDA-TR-104806-005, October 1977, R&D Associates, Santa Monica, CA (in draft).
5. S. A. Kiger, "Instructure Shock Environment of Buried Structures Subjected to Blast Induced Ground Shock," The Shock and Vibration Bulletin, Part 4 of Bulletin 47, September 1977.
6. R. D. Crowson and S. A. Kiger, "The Effect of Earth Cover on the Dynamic Response of Hardened Reinforced Concrete Structures," The Shock and Vibration Bulletin, Part 4 of Bulletin 47, September 1977.
7. J. E. Windham and J. O. Curtis, "Effect of Backfill Properties and Airblast Variations on the External Loads Delivered to Buried Box Structures," Technical Report, U. S. Army Engineer Waterways Experiment Station, Vicksburg, MS (in publication).
8. J. Isenberg, H. S. Levine, and S. H. Pang, "Numerical Simulation of Forced Vibration Tests on a Buried Arch," DNA Contract Report No. 4281F, 1 March 1977, prepared by Weidlinger Associates under Contract No. 001-76-C-0110.
9. J. D. Haltiwanger, W. J. Hall, and N. M. Newmark, "Approximate Methods for the Vulnerability Analysis of Structures Subjected to the Effects of Nuclear Blast," Report No. U-275-76, 15 June 1976, N. W. Newmark Consulting Engineering Services, Urbana, IL.